Published in final edited form as:
FEMS Microbiol Ecol. 2011 August ; 77(2): 322–332. doi:10.1111/j.1574-6941.2011.01113.x.

The biosynthesis of cyanobacterial sunscreen scytonemin in intertidal microbial mat communities

Emily P. Balskus[1], **Rebecca J. Case**[2], and **Christopher T. Walsh**[1]

[1] Department of Biological Chemistry and Molecular Pharmacology, Harvard Medical School, Boston, MA, USA

[2] Department of Biological Sciences, University of Alberta, Edmonton, AB, Canada

Abstract

We have examined the biosynthesis and accumulation of cyanobacterial sunscreening pigment scytonemin within intertidal microbial mat communities using a combination of chemical, molecular, and phylogenetic approaches. Both laminated (layered) and non-laminated mats contained scytonemin, with morphologically distinct mats having different cyanobacterial community compositions. Within laminated microbial mats, regions with and without scytonemin had different dominant oxygenic phototrophs, with scytonemin-producing areas consisting primarily of *Lyngbya aestuarii* and scytonemin-deficient areas dominated by a eukaryotic alga. The non-laminated mat was populated by a diverse group of cyanobacteria and did not contain algae. The amplification and phylogenetic assignment of scytonemin biosynthetic gene *scyC* from laminated mat samples confirmed that the dominant cyanobacterium in these areas, *L. aestuarii*, is likely responsible for sunscreen production. This study is the first to utilize an understanding of the molecular basis of scytonemin assembly to explore its synthesis and function within natural microbial communities.

Keywords

cyanobacteria; microbial mat; scytonemin; secondary metabolite biosynthesis

Introduction

UV-B and UV-A radiation are harmful to living systems, causing both direct and indirect damage to important macromolecules. UV is a particularly serious threat to phototrophic organisms, as they require visible light exposure to fuel their growth and metabolism. Cyanobacteria are photosynthetic microbes with potentially ancient origins that have evolved multiple methods for dealing with the consequences of UV exposure. These strategies include the expression of DNA repair enzymes (Levine & Thiel, 1987), the production of antioxidant enzymes (Shibata, *et al.*, 1991), UV avoidance behavior (Bebout & Garcia-Pichel, 1995), and the synthesis and accumulation of small molecule sunscreens (Cockell & Knowland, 1999). These strategies are especially important for the survival of cyanobacteria in environments exposed to high levels of solar irradiance, such as desert soils, rocks, and shallow marine intertidal areas.

Scytonemin is a small molecule sunscreen that is widely distributed among cyanobacteria from diverse habitats. It is a lipophilic, yellow-brown pigment with a unique, highly

Correspondence: Emily P. Balskus, Department of Biological Chemistry and Molecular Pharmacology, Harvard Medical School, 240 Longwood Ave, Boston, MA 02115, USA. Tel: 617-921-9554; fax: 617-432-0556; emily_balskus@hms.harvard.edu.

conjugated heterocyclic skeleton (Figure 1a) (Proteau *et al.*, 1993). Scytonemin is synthesized in response to UV-A exposure and accumulates within the extracellular sheath or slime of the producing organism, forming a stable, protective layer that absorbs as much as 90% of further incident radiation (λ_{max} = 370 nm *in vivo*, 384 nm *in vitro*) (Garcia-Pichel & Castenholz, 1991). The pigment can constitute up to 5% of cyanobacterial dry weight in cultured organisms and can accumulate at high levels in natural assemblages (Karsten *et al.*, 1998). Scytonemin is often found in the upper layers of microbial mats, which are dense communities of microorganisms that develop in light-exposed areas and are often found in extreme environments.

The gene cluster responsible for scytonemin biosynthesis in the filamentous, heterocystous cyanobacterium *Nostoc punctiforme* was identified in 2007 (Soule *et al.*, 2007). This disclosure has been followed by a series of studies seeking to understand the regulation of biosynthetic gene expression (Soule *et al*, 2009; Sorrels *et al*., 2009) and to elucidate the molecular logic underlying pigment assembly (Balskus & Walsh, 2008; 2009). Our work in the latter area began with the development of a biosynthetic hypothesis (Fig. 1b) and has culminated in the *in vitro* characterization of three scytonemin biosynthetic enzymes, ScyA-C. ScyB converts L-tryptophan to 3-indole pyruvic acid, which is subsequently coupled with *p*-hydroxyphenylpyruvic acid by ScyA, a thiamin-dependent enzyme. The resulting β-ketoacid product is cyclized by ScyC, an enzyme that had been annotated as a hypothetical protein (Soule *et al.*, 2007). This unusual enzymatic transformation produces a tricyclic ketone resembling half of the scytonemin skeleton. We hypothesize that this product is subsequently elaborated to the natural product via several oxidative transformations, including a dimerization reaction that would assemble the entire carbon framework.

The discovery of the genetic basis of scytonemin biosynthesis and continuing investigations into the chemical and regulatory mechanisms underlying pigment assembly have yielded important insights regarding the function of this important natural product in a single producing organism. These efforts have also laid the groundwork for explorations of pigment synthesis by natural cyanobacterial communities using molecular techniques; however, there have been no such studies reported to date. Here we detail our investigations of scytonemin biosynthesis in a natural population using culture-independent methods. Specifically, we have evaluated scytonemin production in three microbial mats from the Little Sippewissett Salt Marsh in Falmouth, MA and have discovered correlations between pigment synthesis and cyanobacterial community composition. We have also amplified and characterized scytonemin biosynthetic gene *scyC* from areas with scytonemin accumulation and used this sequence to identify a likely cyanobacterial producer within the mat community.

Materials and Methods

Mat samples

The microbial mats were located in the Little Sippwissett Salt Marsh near Wood Neck Beach in Falmouth, MA, USA. Scytonemin analysis and sample collection were carried out on October 11, 2010 at 8 AM, approximately one hour after low tide. Mats 1 (41° 34′ 32.42″ N, 70° 38′ 13.36″ W) and 5 (41° 34′ 33.76″ N, 70° 38′ 13.43″ W) were both large, leathery upper intertidal mats with layered structures similar to those of microbial mats located in nearby Great Sippewissett Salt Marsh. The Great Sippewissett mats have previously been studied in detail (Pierson *et al.*, 1987; Nicholson *et al*., 1987). In brief, upper mat layers (0–3 mm) are characteristically gold or dark green in color and are typically dominated by cyanobacteria and diatoms. Lower layers (3–6 mm) may be pink or peach in color and largely contain purple sulfur bacteria. There may also be a layer of green sulfur bacteria (6–7 mm). Layers of black and dark grey sulfidic sand lie below the mat, reaching depths of up

to 50 mm. The upper layers of the two Little Sippewissett mats (Mats 1 and 5) were heterogeneous in appearance, with tough, leathery black to dark green areas interspersed among softer, felt-like, green-gold regions. Thin layer chromatography (TLC) analysis of acetone extracts of mat samples revealed scytonemin in the darker regions of both mats (samples 1A and 5) but not in the lighter regions (sample 1B). Multiple samples from the light and dark regions of both mats were evaluated by TLC to confirm qualitatively that morphology correlated with pigment distribution. Dark pigmentation was also noted on the surface of Mat 6 (41° 34′ 33.80″ N, 70 ° 38′ 27.35″ W), a non-laminated mat or soil crust in the early stages of formation along the sand bordering the tidal inlet, and TLC analysis confirmed the presence of scytonemin. Duplicate core samples were taken for DNA extraction (~10 mm in depth encompassing all of the mat layers) in sterile 15 mL falcon tubes at each mat location. For Mat 1, duplicate cores were taken from both scytonemin producing (sample 1A) and deficient (sample 1B) regions. Samples for large-scale scytonemin extractions were collected in sterile 50 mL falcon tubes and stored at −20 °C.

Thin layer chromatographic (TLC) analysis of scytonemin in the field

This procedure was adapted for the field from a previously reported TLC analysis of scytonemin and reduced scytonemin (Garcia-Pichel & Castenholz, 1991). Small samples of mat (25–50 mg) were transferred to 0.5-dram glass vials using the tip of a clean metal spatula. Acetone (~ 0.5–1.0 mL) was added to each vial and the mat material was pulverized with the tip of a glass Pasteur pipette until the acetone was dark in color. Extracts containing scytonemin were characteristically brown in color, while extracts lacking scytonemin were green. The presence or absence of scytonemin in all samples was confirmed by TLC analysis on silica gel plates (Analtech, Newark, DE) using an eluent of 1:9 methanol:chloroform (R_f ~ 0.4). Scytonemin and its reduced form separate using these conditions and may be recognized by their characteristic colors; the fully oxidized pigment is green-brown in color, while the reduced form is bright red. Extract samples were also co-spotted with and run alongside an acetone solution containing an authentic sample of scytonemin (EMD Chemicals, Merck KGaA, Darmstadt, Germany). Duplicate samples from each mat location were analyzed to confirm the presence or absence of pigment. *Note: organic solvents such as chloroform and methanol are toxic, flammable, and potentially hazardous to the environment; all manipulations involving organic solvents were performed while wearing nitrile gloves and within a secondary container to prevent contact with the surrounding marsh.*

Scytonemin extraction from mat samples

Frozen material from Mat 1 was dried in a 60 °C oven overnight in a large evaporating dish (dry weight = 2.59 g). The sample was ground to homogeneity in 30 mL of acetone in a dark fume hood and allowed to extract at 4 °C in the dark for 8.5 h. The resulting brown extract was clarified by filtration through a Whatman GF/F glass microfiber filter, evaporated using a rotovap, and further dried on a vacuum manifold for 30 min. The residue was triturated with 6 × 2 mL anhydrous pentane to remove carotenoids and chlorophyll; the yellow-green pentane solution was removed and set aside, leaving behind a dark brown-black residue (2.7 mg, 0.1% of dry mat weight) which was dried on a vacuum manifold and stored at −20 °C in the dark. ^{1}H NMR characterization of this material showed a mixture of the oxidized and reduced forms of scytonemin (1:8 ratio). This isolation procedure was repeated for samples from Mats 5 and 6; scytonemin was 0.09% of the dry weight of Mat 5 (1:12 scytonemin:reduced scytonemin) and 0.03% of the dry weight of Mat 6 (1:1.8 scytonemin:reduced scytonemin).

Scytonemin—^{1}H NMR (600 MHz, acetone-d^6)δ: 8.77 (d, 4H, J = 7.9 Hz), 7.66–7.62 (m, 6H), 7.59 (dd, 2H, J = 7.4, 7.4 Hz), 7.23 (dd, 2H, J = 7.6, 7.6 Hz), 7.07 (d, 4H, J = 8.2 Hz). UV absorption spectrum (dimethylsulfoxide): λ_{max} = 384 nm, ε = 16,200 $M^{-1}cm^{-1}$

Reduced scytonemin—^{1}H NMR (600 MHz, acetone-d^6)δ: 10.75 (br s, 2H), 7.77 (d, 4H, J = 8.2 Hz), 7.76 (d, 2H, J = 7.1 Hz), 7.53 (d, 2H, J = 8.0 Hz), 7.41 (s, 2H), 7.27 (dd, 2H, J = 7.6, 7.6 Hz), 7.19 (dd, 2H, J = 7.6, 7.6 Hz), 7.01 (d, 4H, J = 8.6 Hz). UV absorption spectrum (dimethylsulfoxide): λ_{max} = 384 nm, ε = 14,300 $M^{-1}cm^{-1}$

Molecular analysis: cyanobacterial 16S clone libraries

Nucleic acid extractions were performed for each mat sample using the PowerSoil DNA Isolation Kit (Mo Bio Laboratories, Carlsbad, CA) on the same day as collection using 250–300 mg wet weight of each sample. DNA concentrations were determined using a NanoDrop 1000 spectrophotometer (Thermo Scientific, Waltham, MA).

PCR amplification of cyanobacterial and chloroplast 16s rRNA genes was performed using previously reported specific primers CYA359F and CYA781R (Nübel *et al.*, 1997) on all of the DNA samples. PCR reactions contained 12.5 μL of PfuTurbo Hotstart master mix (Strategene), 10 ng of DNA template, and 50 pmoles of each primer in a total volume of 25 μL. Thermocycling was carried out in a MyCycler gradient cycler (Bio-Rad) using the following parameters: denaturation for 2 min at 94 °C, followed by 30 cycles of 1 min at 94 °C, 1 min at 60 °C, 1 min at 70 °C, and a final extension time of 6 min at 70 °C. PCR reactions were analyzed by agarose gel electrophoresis with ethidium bromide staining.

PCR products from replicate DNA samples were pooled and ligated into the pCR4Blunt-TOPO vector using the Zero Blunt TOPO PCR Cloning Kit (Invitrogen) according to the manufacturers protocol. Clone libraries of 100–200 clones were created for each site (four libraries total), and 48 clones from each library were selected for sequencing. Plasmid DNA isolation, purification, and sequencing were performed by the DNA sequencing core at the Bioolymers Facility at Harvard Medical School, Boston, MA, USA. Unsuccessful sequencing reactions were discarded, reducing the size of some of the libraries (library 1A = 42 clones, library 1B = 43 clones, library 5 = 48 clones, library 6 = 41 clones).

Molecular analysis: *scyC* gene libraries

Degenerate PCR primers for the *scyC* gene family were designed by aligning the amino acid sequences of seven ScyC homologs, found by pBLAST searching with the amino acid sequence of ScyC from *Nostoc punctiforme* ATCC 29133, with ClustalW. Two conserved regions were targeted for primer design:

Forward primer (VYFHW): 5′ GTNTAYTTYCAYTGG 3′

Reverse primer (MNIKR): 5′ ADCKYTTDATRTTCAT 3′

PCR reactions contained 12.5 μL of PfuTurbo Hotstart master mix, 10 ng of DNA template, and 100 pmoles of each primer in a total volume of 25 μL. Thermocycling was carried out in a MyCycler gradient cycler (Bio-Rad) with an initial denaturation period of 1 min at 95 °C, followed by 10 cycles of 30 sec at 95 °C, 1 min at 46.2 °C and 1 min at 72 °C, followed by 44 cycles of 30 sec at 95 °C, 1 min at 43.6 °C, 1 min at 72 °C, and a final extension time of 5 min at 72 °C. PCR reactions were analyzed by agarose gel electrophoresis with ethidium bromide staining. Bands of the expected length (~550 bp) were observed for samples 1A and 5A, but not for samples 1B or 6. Amplified products from duplicate samples from 1A and 5A were pooled and further purified using agarose gel electrphoresis and the Illustra GFX PCR DNA and Gel Band Purification Kit (GE Healthcare) prior to cloning.

Purified PCR products were ligated into the pCR4Blunt-TOPO vector using the Zero Blunt TOPO PCR Cloning Kit (Invitrogen) according to the manufacturers protocol. Clone libraries of 100–200 clones were created for each site (two libraries). Before performing extensive sequencing, three clones were picked from each library and sequenced (Molecular Biology Core Facility of the Dana Farber Cancer Institute, Boston, MA) and confirming homology to *scyC*. A further 20 more clones from the 1A and 5A libraries were sequenced in an analogous manner.

Phylogenetic analysis

The phylogenetic tree of the microbial mat 16S rRNA gene clone libraries and the *scyC* translated sequence were reconstructed using PHYML (Guindon & Gascuel, 2003) with the GTR nucleotide substitution model, the proportion of invariable sites and the gamma parameter of across-site rate variation (using four rate categories) was estimated from the dataset. Bootstrap support values were calculated with the same parameters (100 replicates). The sequence datasets used for the analysis is a combination of all sequences obtained from the microbial mats (16S rRNA gene or *scyC*), their closest BLAST hits from the Genbank nucleotide, genome and environmental databases. These were aligned using ClustalX (Thompson *et al*., 1994) and manually edited to a final length of 409 bp for the 16S rRNA gene and 530 aa for ScyC.

The software package Mothur (Schloss *et al*., 2009) was used for all richness and diversity analyses of the four 16S rRNA gene clone libraries sequenced. Operational taxonomic units (OTU) were defined as sequences sharing 98% sequence identity (Gevers *et al.*, 2005) for these analyses (clustered using the nearest neighbor algorithm) ($OTU_{0.02}$). Rarefaction curves were compiled for the cyanobacterial sequences of the three largest libraries with the default parameters, excluding the penalty for terminal gaps while compiling the distance matrices. Confidence intervals were determined at the 95% level. Total OTU richness was also calculated for the cyanobacterial component of each of these libraries using the Chao1 estimator. The similarity between the four clone libraries (including chloroplastic sequences) is represented as an UPGMA dendrogram based on distance matrices for the Yue & Clayton theta index (Schloss *et al*., 2009). A venn diagram was also drawn to depict the number of $OTU_{0.02}$ shared by all four libraries (including chloroplastic sequences).

Nucleotide sequence accession numbers

Sequences from these experiments were deposited in GenBank under accession numbers HQ124097 to HQ124272.

Results

Microbial mats are dense assemblages of microbes that form in light-exposed areas, typically in marine intertidal, hot spring, or hypersaline environments (Franks & Stoz, 2009). Typically containing large numbers of photosynthetic organisms, these mats can be important sources of primary production and may contribute to sediment formation and stabilization. The cyanobacterial sunscreen scytonemin is often found in the upper layers of microbial mats, where it is thought to play an important role in protecting the inhabitants of these zones from harmful UV-A radiation (Karsten *et al.*, 1998).

We chose to study scytonemin production in microbial mats from the Little Sippewissett Salt Marsh in Falmouth, MA, USA (Fig. 2). The location of scytonemin within the top layers of individual mats was pinpointed using thin-layer chromatography (TLC) experiments in the field. We found scytonemin production in mats with two distinctive morphologies. The first mat type (exemplified by Mats 1 and 5) had an organized, layered

structure typical of well-studied mats from the nearby Great Sippewissett Salt Marsh. The surfaces of these mats were also notable for their heterogeneous appearance, with dark green leathery patches interspersed among less cohesive, lighter green areas (Fig. 2c). Scytonemin was detected only in extracts from the dark green regions of the mat, and was found only in its oxidized form; extracts from other areas of the mat did not contain scytonemin.

The other scytonemin-producing microbial mat we identified (Mat 6) was non-laminated and appeared to be at an early stage of development (Fig. 2d). Its sandy surface was uneven and mostly brown in color, with some areas of intense orange pigmentation that are likely due to high levels of carotenoid production. Scytonemin was found in all samples taken from this mat, and was especially prevalent in areas with extensive brown pigmentation. In addition to detecting pigment in the field, we also performed large-scale scytonemin extractions from the mats. This provided not only validation of pigment structure, but also an estimate of its relative abundance (Fig. 2e).

The characterization of scytonemin distribution within the Little Sippewissett microbial mats focused our subsequent cyanobacterial community analyses on addressing several questions. In the case of the laminated mats, how would the community composition of a single mat vary between regions with and without scytonemin (samples 1A vs. 1B)? Were the same scytonemin-producing cyanobacteria found in the two morphologically similar but physically distant mats (samples 1A vs. 5)? Finally, how would the community composition compare between two morphologically distinct mats that both contain scytonemin (samples 1A and 5 vs. 6)? Through amplification and phylogenetic analysis of a scytonemin biosynthetic gene from scytonemin-containing samples, we also hoped to identify potential producers within each community.

DNA was extracted from duplicate core samples taken from scytonemin-producing areas of each mat (samples 1A, 5 and 6) as well as from an area of Mat 1 lacking scytonemin (sample 1B). To determine the cyanobacterial community composition at each site, previously described PCR primers (Nübel *et al.*, 1997) were used to amplify a fragment of the 16S rRNA gene for sequencing. This PCR approach specifically amplified both cyanobacterial and chloroplast sequences.

The community compositions of scytonemin-producing areas in laminated mats (samples 1A and 5) were remarkably similar despite their physical separation (Fig. 5a). Both libraries were dominated by 16S rRNA gene sequences from *Lyngbya aestuarii* (18 out of 42 sequences for library 1A and 29 out of 48 sequences for library 5). These sequences, along with 10 other close homologs, form a distinct clade with sequences from cultured *Lyngbya* strains, including *Lyngbya* sp. PCC 8106 (*L. aestuarii*) and *Lyngbya majuscula* (Fig. 4a). The second most abundant group of sequences are related to *Microcoleus chthonoplastes* (Fig. 4). These cyanobacteria have a cosmopolitan distribution and have been found in numerous intertidal microbial mats systems (Garcia-Pichel *et al*., 1996). Interestingly, *M. chthonoplastes*' 16S rRNA gene sequence was found in all scytonemin-containing mat communities. Mat samples 1A and 5 also contained small numbers of cyanobacterial sequences belonging to the genera *Leptolyngbya* and *Chlorogloeopsis*, and a small clade of sequences resembling those retrieved from the metagenome of another microbial mat (Isenbarger *et al.*, 2008; Yannarell *et al.*, 2007). Chloroplast 16S rRNA gene sequences from diatoms were also retrieved from these two libraries (Fig. 4b).

The zones of the layered mat lacking scytonemin (sample 1B) revealed a strikingly different community composition compared to areas with sunscreen. Few cyanobacterial 16S rRNA gene sequences were retrieved from this region of the mat (Fig. 5b), making it impossible to estimate the cyanobacterial diversity. The library also lacked *Lyngbya* sequences. Instead the

16S rRNA gene library was dominated by a single chloroplast sequence (34 out of 43 clones) with 94% sequence identity to that of the yellow-green filmentous algae *Vaucheria litorea* (Xanthophyceae) that is commonly found in intertidal regions (Fig. 4b) (Lee, 1989; Rumpho *et al*., 2008). Apart from the abundant Xanthophyceae sequence, the remaining 16S rRNA gene sequences are from diatoms (Fig. 4B) and three cyanbacteria (Fig. 3).

Distinct cyanobacterial communities were also found when comparing the layered scytonemin producing mats (samples 1A and 5) to the morphologically distinct, non-laminated scytonemin-containing mat (sample 6). The non-laminated mat community was composed entirely of cyanobacterial 16S rRNA gene sequences, with no dominant sequence (Fig. 3); rarefraction curves (Fig. 5C) and the resulting Chao diversity estimate indicated this sample had the highest cyanobacterial diversity (sample 6B: 41 (low 95% CI 29, high 95% CI 84), sample 5A: 21 (low 95% CI 12, high 95% CI 64) and sample 1A: 17 (low 95% CI 13, high 95% CI 41)). In addition to *M. chthonoplastes* the non-laminated mat also contained multiple filamentous cyanbacteria, heterocystous strains and *Leptolyngbya* sp. but interestingly no *Lyngbya* or chloroplast sequences (Fig. 3).

A single scytonemin biosynthetic gene sequence was retrieved from the scytonemin-containing areas of both layered mats (samples 1A and 5), whereas no products of the anticipated size amplified from zones lacking scytonemin (sample 1B) or from the non-laminated scytonemin-containing mat (sample 6B). The gene encoding indole cyclizing enzyme *scyC* was chosen as a target for amplification by degenerate PCR due to its strict association with scytonemin gene clusters and does not share homology with other enzyme sequences. Other genes in the scytonemin cluster are related to primary metabolic enzymes or are homologous to other genes within the same cluster, which makes their selective amplification problematic. There is sequence diversity among *scyC* genes from different cyanobacteria (52% aa identity within this gene family) making it possible to assess the phylogeny of *scyC* sequences isolated from the environment.

Interestingly, all of the *scyC* sequences retrieved from the Little Sippwissett Salt Marsh were identical at the nucleotide level. Comparison of these environmental sequences with the NCBI database revealed they had > 99% sequence identity at the nucleotide level to *scyC* from *Lyngbya* sp. PCC 8106 (*L. aestuarii*). This relationship was confirmed by constructing a maximum-likelihood phylogenetic tree of the mat sequences with the six *scyC* sequences in the database (Fig. 6). This result provides strong evidence that *L. aestuarii* is the dominant cyanobacterial species in the scytonemin-containing regions of Mats 1 and 5 (Fig. 4A), and that it is also the major producer of scytonemin in these microbial communities (Fig. 6).

Discussion

Our characterization of the cyanobacterial community compositions of microbial mats in the Little Sippewissett Salt Marsh has revealed distinct population differences that are linked to sunscreen production and mat morphology. Scytonemin biosynthesis in laminated mats (Mats 1 and 5) was associated with the presence of a single dominant cyanobacterial species, *Lyngbya aestuarii*. Areas of these mats deficient in scytonemin production completely lacked *Lyngbya* 16S rRNA gene sequences and were instead dominated by eukaryotic algae, with a single chloroplast 16S rRNA gene sequence belonging to the Xanthophyte being the most abundant. The cyanobacterial community of a scytonemin producing non-laminated mat in the early stages of development (Mat 6) was distinct from those of the layered mats, as it contained a more diverse cyanobacterial community lacking both *Lyngbya* and eukaryotic algae.

In the laminated mats, the localization of scytonemin and the gene *scyC*, which is involved in its biosynthesis, in regions with a single dominant cyanbacterial 16S rRNA gene sequence suggested that this organism, *L. aestuarii*, might be responsible for sunscreen production. This hypothesis is strongly supported by the characterization of a single *scyC* sequence from the producing areas of Mats 1 and 5 that is nearly identical to the *scyC* sequence from *Lyngbya* sp. PCC 8106 (*L. aestuarii)*. Additionally, this result obtained using culture-independent methods is supported by previous reports of the isolation and culturing of scytonemin-producing *Lyngbya* sp. from closely related microbial mats (Garcia-Pichel & Castenholz, 1991; 1993).

Connecting scytonemin biosynthesis to particular cyanobacteria was not possible for Mat 6 due to our inability to amplify *scyC* sequences. Since Mat 6 is not dominated by a single producing organism, the amount of template DNA encoding scytonemin biosynthetic genes could be much less concentrated relative to samples from Mats 1 and 5. Also, the scytonemin-producing cyanobacteria in Mat 6 are likely only distantly related to producing organisms whose biosynthetic genes have been sequenced, which could render the degenerate PCR reaction ineffective. Finally, there is the possibility that the cyanbacterial community has undergone succession and the organism(s) originally responsible for pigment production in this community are no longer present.

The presence of a single, dominant scytonemin-producing cyanobacterium in the laminated microbial mats is intriguing and may have important implications for the entire community. Culture- and microscopy-based methods have revealed similar scenarios in other intertidal mats (Karsten *et al*., 1998) and biofilm communities (Branowitz & Castenholz, 1997), suggesting that sunscreen biosynthesis may provide organisms with a competitive advantage in these environments. The ability to block harmful radiation should allow sunscreen-producing phototrophs more light exposure relative to their non-producing counterparts, which may fuel more rapid growth. But it is important to note that high levels of sunscreen accumulation by a single dominant organism or group of organisms may also benefit the entire community; initial filtering of harmful radiation by the scytonemin producer would reduce the exposure of all organisms residing in the upper mat layers, with the accompanying tradeoff for other phototrophs being less access to visible light.

Microbes present in the lower mat layers may have the potential to influence the chemical structure of scytonemin. Although we detected only the fully oxidized form of scytonemin in the field, pigment extracted from mat samples was found to be largely in the reduced form. The conversion of scytonemin to reduced scytonemin likely occurs upon sample collection and storage, when the upper levels of the mat are exposed to the lower mat layers within sealed tubes in the absence of light. The lower portion of these microbial mats contains sulfate-reducing bacteria, which produce elemental sulfur and hydrogen sulfide as byproducts of their metabolism. As hydrogen sulfide and sodium sulfide are both capable of converting scytonemin to its reduced form (Garcia-Pichel & Castenholz, 1991), the isolation of primarily reduced scytonemin from collected mat samples suggests this redox process may have ecological relevance where there is mixing of the mat layers or diffusion over gradients. The oxygen and sulfide gradient profiles within laminated microbial mats have been well characterized; organisms in upper mat layers are regularly exposed to sulfide, particularly at night when photosynthesis has ceased (Franks & Stolz, 2009). Sulfide is typically harmful to cyanobacteria, as it inhibits oxygenic photosynthesis (Oren *et al.*, 1979). We suggest that another important but underappreciated role of scytonemin accumulation may be to protect producing organisms by consuming toxic sulfide in a redox reaction. This reduction should not compromise scytonemin's sunscreening properties, as the λ_{max} of reduced scytonemin is unchanged from the oxidized form and the extinction coefficients of the two pigments are comparable (see characterization in Materials and Methods).

Additionally, the reduction of scytonemin by sulfide should be reversed with exposure to oxygen or perhaps also by enzymatic oxidation (Figure 1a). The reversible nature of the scytonemin redox may therefore constitute an important adaptation for life in the dynamic mat environment where redox chemistry defines the layered niches within the mat community.

A distinctive feature of the Little Sippewissett laminated mats relative to previously described systems is the uneven distribution of the major phototrophic organisms in their upper layers. The presence of eukaryotic algae and cyanobacteria within the same mat raises important questions about competition exclusion within these ecosystems. As oxygenic phototrophs, cyanobacteria and algae have the same major chlorophyll pigment (chl *a*) and are direct competitors for light and resources. The uneven distribution of these phototrophs between samples may be indicative of competition for resources or of an allelopathic relationship wherein one or both organisms inhibits the growth of the other through the production of bioactive small molecules (Gross, 2003). The production of algicidal compounds by cyanobacteria was described as early as 1917 (Harder), and since then many examples of allelopathy among cyanobacteria or between cyanobacteria and algae have been characterized using cultured organisms (Leão *et al*., 2009; Leão *et al*., 2010; Berry *et al*., 2008; Smith & Doan, 1999). In the field, evidence for allelopathy has been found primarily among freshwater bloom-forming cyanobacteria (Leão *et al*., 2009; Keating, 1977 and 1978); our observations suggest that these interactions may also be important in shaping microbial mat communities. *Lyngbya* species, especially *Lyngbya majuscula*, are prolific producers of secondary metabolites (Jones *et al.*, 2009). Though comparatively few secondary metabolites have been characterized from *L. aestuarii*, isolation of an herbicidal polyketide natural product has been reported (Entzeroth *et al*., 1985). Characterization of community composition over time, as well as examination of the behavior of the dominant cyanobacteria and algae in co-culture will be an important next steps in determining the exact nature of their interaction.

The lack of any scytonemin production in algae-dominated regions of the laminated mats suggests that these organisms utilize an alternate mechanism of UV protection. The synthesis of mycosporines and mycosporine-like amino acids (MAAs), a family of UV-absorbing small molecules, is widespread among algae (Gröniger, 2000). In combination with other defense mechanisms, the accumulation of these alternative sunscreens could be another important factor allowing the algal species in the laminated mats to compete effectively with *L. aestuarii*.

Comparison of the cyanobacterial community compositions of laminated and non-laminated mats revealed important differences in community structure between these habitats. The non-laminated scytonemin-containing Mat 6 did not contain eukaryotic algae and was the most diverse with respect to the Chao diversity estimate (41 (low 95% CI 29, high 95% CI 84)) and phylogeny of cyanobacterial species (Fig 3 & 5). The lack of a dominant 16S rRNA gene sequence within this mat might be a consequence of lower nutrient availability and harsher conditions, as mats in early stages of development are typically less productive and therefore more oligotrophic environments (Stal, 1984). The interesting observation that scytonemin levels are still high in this mat despite its greater cyanobacterial diversity and apparent lack of a scytonemin producer could indicate that many of these cyanobacteria are capable of sunscreen production and that this environment selects for organisms with this trait. As scytonemin has been observed in members of all cyanobacterial taxa, this hypothesis is appealing, but further data linking pigment biosynthesis to individual species using either microscopy or molecular techniques will be required for confirmation.

Our investigations of scytonemin biosynthesis in the Little Sippewissett Salt Marsh microbial mats are the first to employ molecular techniques to study the synthesis of this important sunscreen in natural cyanobacterial populations. We have found striking differences in cyanobacterial community composition associated with pigment production and mat morphology. In layered communities, scytonemin biosynthesis can be reliably linked to a single dominant cyanobacterium, *L. aestuarii*, which may compete with a dominant eukaryotic algal species in the mat's upper layers. Remarkably, this community structure was nearly identical in two morphologically similar but physically separate mats. In a non-laminar scytonemin-containing mat no single cyanobacterium dominated and production could not be assigned to any member of its cyanbacterial community. Both mat communities offer interesting avenues for future investigations into the ecological importance of scytonemin biosynthesis and the roles of particular scytonemin producing organisms within natural assemblages.

Acknowledgments

This work is supported by the National Institutes of Health (GM20011). E. P. B. is the recipient of an NIH postdoctoral fellowship and R.J.C. is supported by the Office of Naval Research (N000141010447). We thank Dr. Hinsby Castillo (University of Illinois Champaign-Urbana), Anne Dekas (California Institute of Technology), and Professor Daniel Buckley (Cornell University) for helpful discussions.

References

Balskus EP, Walsh CT. Investigating the initial steps in the biosynthesis of cyanobacterial sunscreen scytonemin. J Am Chem Soc. 2008; 130:15260–15261. [PubMed: 18954141]

Balskus EP, Walsh CT. An enzymatic cyclopentyl[*b*]indole formation involved in scytonemin bisynthesis. J Am Chem Soc. 2009; 131:14648–14649. [PubMed: 19780555]

Bebout BM, Garcia-Pichel F. UV-B induced vertical migrations of cyanobacteria in a microbial mat. Appl Eviron Microbiol. 1995; 61:4215–4222.

Berry JP, Gantar M, Perez MH, Berry G, Noriega FG. Cyanobacterial toxins as allelochemicals with potential applications as algaecides, herbicides, and insecticides. Mar Drugs. 2008; 6:117–146. [PubMed: 18728763]

Branowitz S, Castenholz R. Long-term effects of UV and visible irradiance on natural populations of a scytonemin-containing cyanobacteriam (*Calothrix* sp.). FEMS Microbiol Ecol. 1997; 24:343–352.

Cockell CS, Knowland J. Ultraviolet radiation screening compounds. Biol Rev. 1999; 74:311–345. [PubMed: 10466253]

Entzeroth M, Mead DJ, Patterson GML, Moore RE. A herbicidal fatty acid from *Lyngbya aestuarii*. Phytochemistry. 1985; 24:2875–2976.

Franks J, Stolz JF. Flat laminated microbial mat communities. Earth-Science Reviews. 2009; 96:163–172.

Garcia-Pichel F, Castenholz R. Characterization and biological implications of scytonemin, a cyanobacterial sheath pigment. J Phycol. 1991; 27:395–409.

Garcia-Pichel F, Castenholz R. Occurance of UV-absorbing, mycosporine-like compounds among cyanobacterial isolates and an estimate of their screening capacity. Appl Environ Microbiol. 1993; 59:163–169. [PubMed: 16348839]

Garcia-Pichel F, Bebout PL, Muyzer G. Phenotypic and phylogenetic analysis show *Microcoleous chthonoplastes* to be a cosmopolitan cyanobacterium. Appl Environ Microbiol. 1996; 62:3284–3291. [PubMed: 8795218]

Gevers D, Cohan FM, Lawrence JG, et al. Re-evaluating prokaryotic species. Nat Rev Microbiol. 2005; 3:733–739. [PubMed: 16138101]

Gröniger A, Sinha RP, Klisch M, Häder D-P. Photoprotective compounds in cyanobacteria, phytoplankton and macroalgae a database. J Photochem Photobiol B. 2000; 58:115–122. [PubMed: 11233638]

Gross EM. Allelopathy of aquatic autotrophs. Crit Rev Plant Sci. 2003; 22:313–339.

Guindon S, Gascuel O. A simple, fast, and accurate algorithm to estimate large phylogenies by maximum likelihood. Systematic Biology. 2003; 52:696–704. [PubMed: 14530136]

Harder R. Physiological nutrition studies of cyanobacteria, mainly the endophytic *Nostoc punctiforme*. Zeitschrift für Botanik. 1917; 9:145–242.

Isenbarger TA, Finney M, Ríos-Velázquez C, Handelsman J, Ruvkun G. Miniprimer PCR, a new lens for viewing the microbial world. Appl Environ Microbiol. 2008; 74:840–849. [PubMed: 18083877]

Jones AC, Gu L, Sorrels CM, Sherman DH, Gerwick WH. New tricks from ancient algae: natural product biosynthesis in marine cyanobacteria. Curr Opin Chem Biol. 2009; 13:216–223. [PubMed: 19307147]

Karsten U, Maier J, Garcia-Pichel F. Seasonality in UV-absorbing compounds of cyanobacterial mat communities from an intertidal mangrove flat. Aquat Microb Ecol. 1998; 16:37–44.

Keating KI. Allelopathic influence on blue-green sequence in a eutrophic lake. Science. 1977; 196:885–887. [PubMed: 17821808]

Keating KI. Blue-green algal inhibition of diatom growth: transition from mesotrophic to eutrophic community structure. Science. 1978; 199:971–973. [PubMed: 17752367]

Leão PN, Vasconcelos TSD, Vasconcelos VM. Allelopathy in freshwater cyanobacteria. Crit Rev Microbiol. 2009; 35:271–282. [PubMed: 19863381]

Leão PN, Periera AR, Liu W, et al. Synergistic allelochemicals from a freshwater cyanobacterium. Proc Natl Acad Sci USA. 2010; 107:11183–11188. [PubMed: 20534563]

Lee, RE. Phycology. Lee, RE., editor. Cambridge University Press; Cambridge: 1989. p. 507-522.

Levine E, Thiel T. UV-inducible DNA repair in the cyanobacteria *Anabaena* spp. J Bacteriol. 1987; 169:3988–3993. [PubMed: 3114232]

Nicholson JM, Stolz JF, Pierson BK. Structure of a microbial mat at Great Sippewissett Marsh, Cape Cod, Massachussetts. FEMS Microbiol Ecol. 1987; 45:343–364.

Nübel H, Garcia-Pichel F, Muyzer G. PCR primers to amplify 16S genes from cyanobacteria. Appl Environ Microbiol. 1997; 63:3327–3332. [PubMed: 9251225]

Oren A, Padan E, Malkin S. Sulfidic inhibition of photosystem II in cyanobacteria (blue-green algae) and tobacco chloroplasts. Biochem Biophys Acta. 1979; 546:270–279. [PubMed: 109120]

Pierson B, Oesterle A, Murphy GL. Pigments, light penetration, and photosynthetic activity in the multi-layered microbial mats of Great Sippewissett Salt Marsh, Massachussetts. FEMS Microbiol Ecol. 1987; 45:365–376.

Proteau PJ, Gerwick WH, Garcia-Pichel F, Castenholz R. The structure of scytonemin, an ultraviolet sunscreen pigment from the sheaths of cyanobacteria. Experientia. 1993; 49:825–829. [PubMed: 8405307]

Rumpho ME, Worful JM, Lee J, Kannan K, Tyler MS, Bhattacharya D, Moustafa A, Manhart JR. Horizontal gene transfer of the algal nuclear gene *psbO* to the photosynthetic sea slug *Elysia chlorotica*. Proc Natl Acad Sci USA. 2008; 105:17867–17871. [PubMed: 19004808]

Schloss PD, Wescott SL, Ryabin T, et al. Introducing mothur: open-source, platform-independent, community-supported software for describing and comparing microbial communities. Appl Environ Microbiol. 2009; 75:7537–7541. [PubMed: 19801464]

Shibata H, Baba K, Ochiai H. Near-UV induces shock proteins in *Anacystis nidulans* R-2: possible role of active oxygen. Plant Cell Physiol. 1991; 32:771–776.

Smith GD, Doan NT. Cyanobacterial metabolites with bioactivity against photosynthesis in cyanobacteria, algae and higher plants. J Appl Phycol. 1999; 11:337–344.

Soule T, Stout V, Swingley WD, Meeks JC, Garcia-Pichel F. Molecular genetics and genomic analysis of scytonemin biosynthesis in *Nostoc punctiforme* ATCC 29133. J Bacteriol. 2007; 189:4465–4472. [PubMed: 17351042]

Soule T, Garcia-Pichel F, Stout V. Gene expression patterms associated with the biosynthesis of the sunscreen scytonemin in *Nostoc punctiforme* ATCC 29133 in response to UV radiation. J Bacteriol. 2009; 191:4639–4646. [PubMed: 19429608]

Sorrels CM, Proteau PJ, Gerwick WH. Organization, evolution, and expression analysis of the biosynthetic gene cluster for scytonemin, a cyanobacterial UV-absorbing pigment. Appl Environ Microbiol. 2009; 75:4861–4869. [PubMed: 19482954]

Stal LJ, Grossberger S, Krumbein WE. Nitrogen fixation associated with the cyanobacterial mat of a marine laminated microbial ecosystem. Mar Biol. 1984; 82:217–224.

Thompson JD, Higgins DG, Gibson TJ. ClustalW - Improving the sensitivity of progressive multiple sequence alignment through sequence weighting, position specific gap penalties and weight matrix choice. Nucleic Acids Research. 1994; 22:4673–4680. [PubMed: 7984417]

Yannarell AC, Steppe TF, Paerl HW. Disturbance and recovery of microbial community structure and function following Hurricaine Francis. Environ Microbiol. 2007; 9:576–583. [PubMed: 17298358]

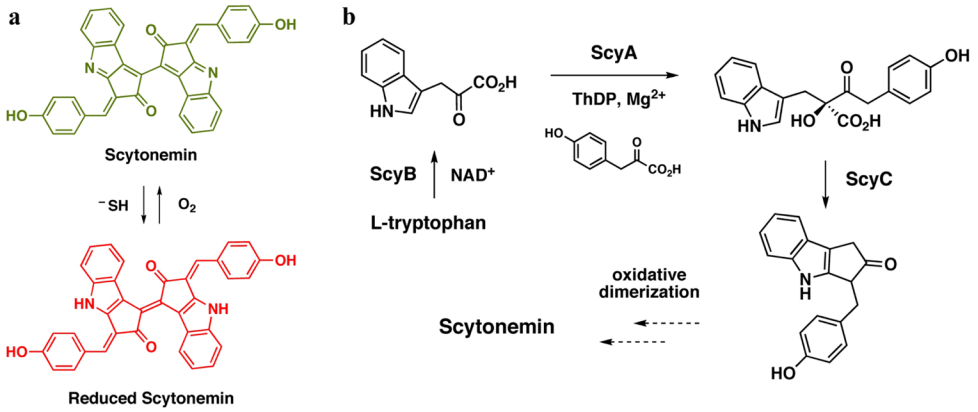

Figure 1.

A) The structures of scytonemin and reduced scytonemin. **B)** Proposed biosynthetic pathway for scytonemin production with biochemically characterized enzymatic transformations.

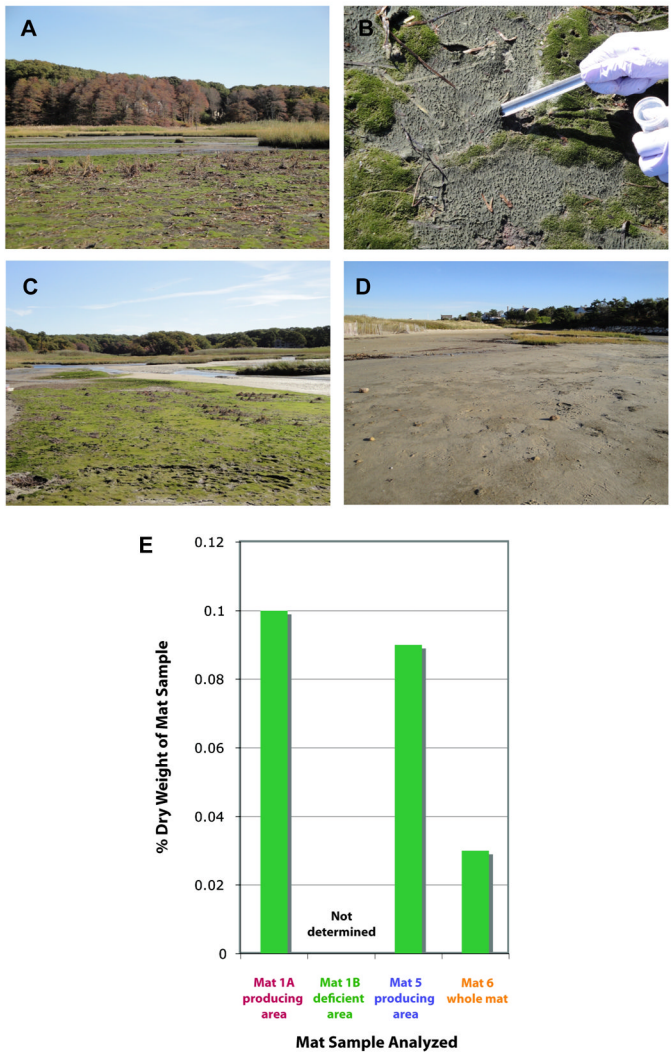

Figure 2.

Photographs of Little Sippewissett microbial mats. **A)** Mat 1 **B)** Detail of Mat 1 surface with dark green, leathery scytonemin-producing areas and lighter green, felt-like areas without scytonemin. **C)** Mat 5 **D)** Mat 6 **E)** Isolated scytonemin from mat samples.

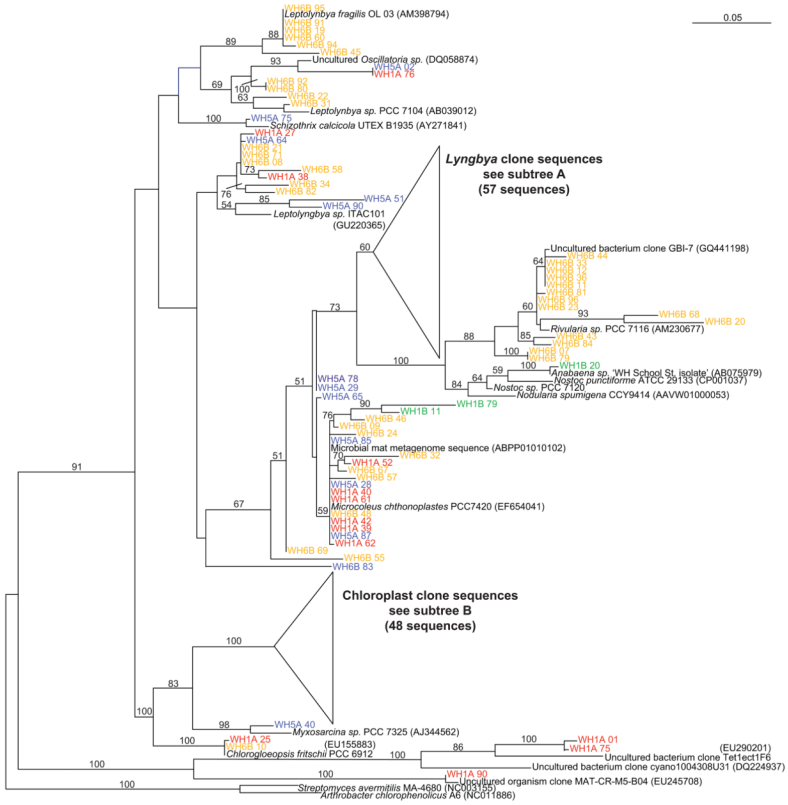

Figure 3.

Maximum likelihood phylogeny of 16S rRNA gene sequences from microbial mats. The tree was compiled by maximum likelihood using PHYML. Bootstrap confidence values >50 are indicated on the nodes. Strains are indicated after species names, followed by the accession number in parenthesis. Sequences are colored according to library (red = Mat 1A [scytonemin producing area], green = Mat 1B [scytonemin deficient area], blue = Mat 5, orange = Mat 6).

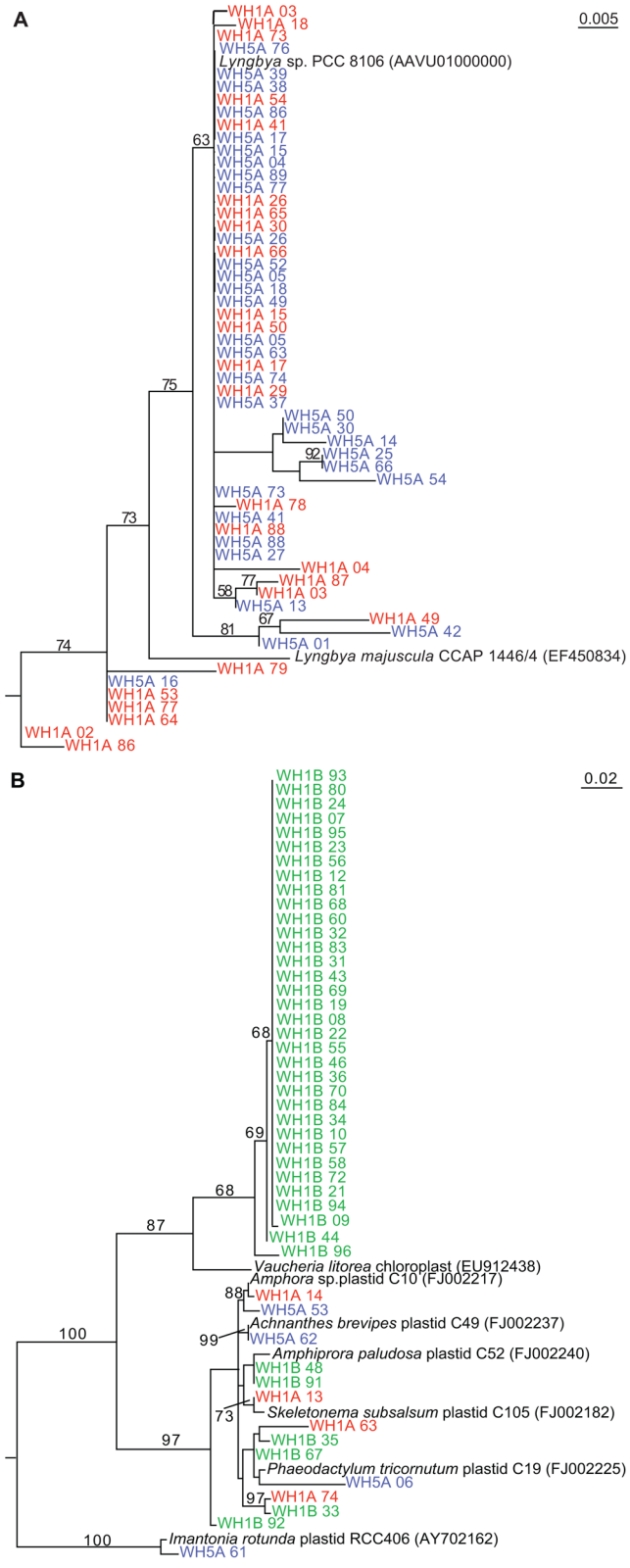

Figure 4.

Maximum likelihood phylogeny of **A)** *Lyngbya* and **B)** chloroplast 16S rRNA gene sequences from microbial mats. The tree was compiled by maximum likelihood using PHYML. Bootstrap confidence values >50 are indicated on the nodes. Strains are indicated after species names, followed by the accession number in parenthesis.

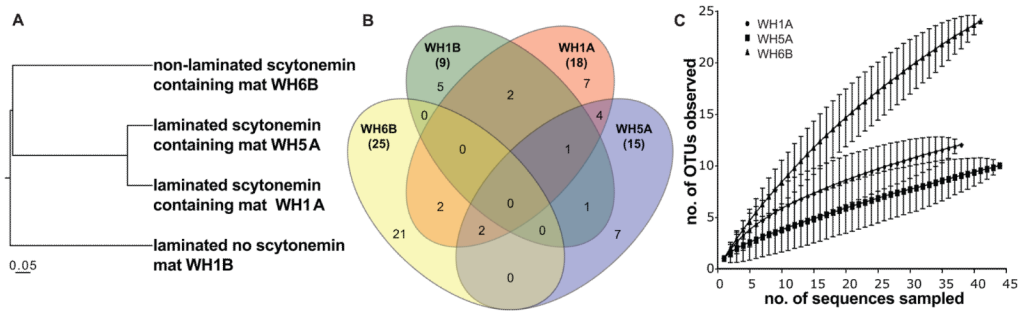

Figure 5.

Richness and diversity analyses of microbial mat 16S rRNA gene clone libraries. The operational taxonomic unit definition used in all analyses corresponds to 98% DNA sequence identity ($OTU_{0.02}$). **A)** UPGMA dendrogram of the similarity between clone libraries (including cyanobacterial and chloroplastic sequences). **B)** Venn diagram representing the number of $OTU_{0.02}$ shared by the clone libraries (including cyanobacterial and chloroplastic sequences). The total number of OTUs in each library is shown in brackets. **C)** Rarefaction curves for the cyanobacterial sequences of the three largest clone libraries. Error bars represent a 95% confidence interval.

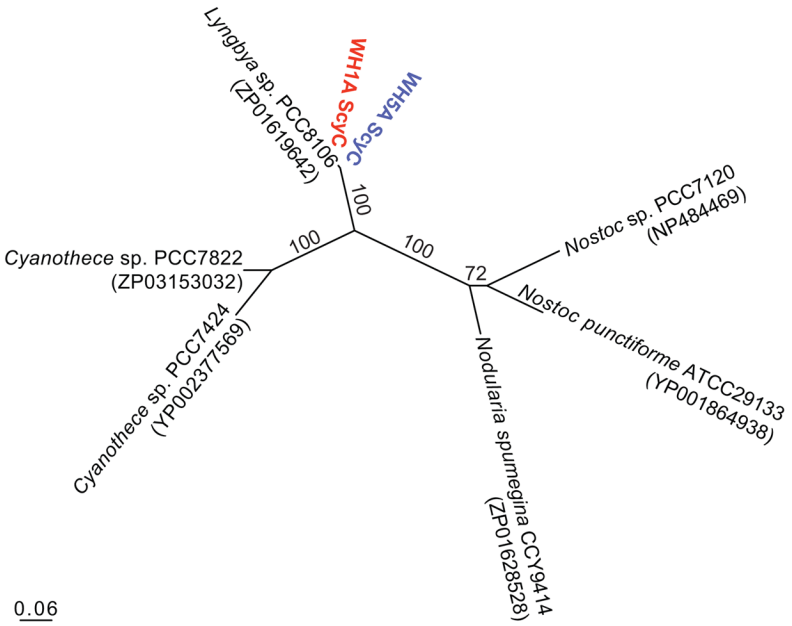

Figure 6.

Maximum likelihood phylogenetic tree of translated ScyC amino acid sequences from sequenced cyanobacteria and Mats 1 and 5. The tree was compiled by maximum likelihood using PHYML. Bootstrap confidence values >50 are indicated on the nodes. The number in parentheses found after each taxon name is the accession number for the respective protein sequence.